

J. Rzadkiewicz, W. Dominik, M. Scholz, K-D. Zastrow, M. Chernyshova,
T. Czarski, H. Czyrkowski, R. Dabrowski, K. Jakubowska, L. Karpinski,
G. Kasprowicz, K. Kierzkowski, K. Pozniak, Z. Salapa, W. Zabolotny,
P. Blanchard, S. Tyrrell and JET EFDA contributors

Novel Design of Triple GEM Detectors for High-Resolution X-Ray Diagnostics on JET

Novel Design of Triple GEM Detectors for High-Resolution X-Ray Diagnostics on JET

J. Rządkiwicz¹, W. Dominik², M. Scholz¹, K-D. Zastrow³, M. Chernyshova¹,
T. Czarski¹, H. Czyrkowski², R. Dabrowski², K. Jakubowska¹, L. Karpinski¹,
G. Kasprowicz⁴, K. Kierzkowski², K. Pozniak⁴, Z. Salapa², W. Zabolotny⁴,
P. Blanchard⁵, S. Tyrrell³ and JET EFDA contributors*

JET-EFDA, Culham Science Centre, OX14 3DB, Abingdon, UK

¹*IPPLM, EURATOM Association, Hery 23, 01-497 Warsaw, Poland*

²*Warsaw University, Faculty of Physics, Institute of Experimental Physics, 00-681 Warsaw, Poland*

³*EURATOM/CCFE Fusion Association, Culham Science Centre, OX14 3DB, Abingdon, UK*

⁴*Warsaw University of Technology, Institute of Electronic Systems, 00-665 Warsaw, Poland*

⁵*Association EURATOM-Confédération Suisse, Ecole Polytechnique Fédérale de Lausanne (EPFL),
CRPP, CH-1015 Lausanne, Switzerland*

* See annex of F. Romanelli et al, "Overview of JET Results",
(23rd IAEA Fusion Energy Conference, Daejeon, Republic of Korea (2010)).

Preprint of Paper to be submitted for publication in Proceedings of the
2nd International Conference Frontiers in Diagnostic Technologies
Frascati, Italy
(28th November 2011 - 30th November 2011)

“This document is intended for publication in the open literature. It is made available on the understanding that it may not be further circulated and extracts or references may not be published prior to publication of the original when applicable, or without the consent of the Publications Officer, EFDA, Culham Science Centre, Abingdon, Oxon, OX14 3DB, UK.”

“Enquiries about Copyright and reproduction should be addressed to the Publications Officer, EFDA, Culham Science Centre, Abingdon, Oxon, OX14 3DB, UK.”

The contents of this preprint and all other JET EFDA Preprints and Conference Papers are available to view online free at www.iop.org/Jet. This site has full search facilities and e-mail alert options. The diagrams contained within the PDFs on this site are hyperlinked from the year 1996 onwards.

ABSTRACT

Upgraded high-resolution x-ray diagnostics on JET is expected to monitor the plasma radiation emitted by W^{46+} and Ni^{26+} ions at 7.8keV and 2.4 keV photon energies, respectively. Both, X-ray lines will be monitored by new generation energy-resolved micropattern gas detectors with 1-D position reconstruction capability. The detection structure is based on triple GEM (T-GEM) amplification structure followed by the strip readout electrode. This article presents a design of new detectors and prototype detector tests.

1. INTRODUCTION

High-resolution X-ray spectroscopy is a powerful tool for diagnosing the properties of tokamak plasmas. The characteristic X-ray radiation emitted by highly ionized metal atoms provides accurate information on crucial plasma parameters related to the impurity concentration, ion temperature and the toroidal rotation velocity [1,2]. The high-resolution spectrometer in the so-called Johann geometry with a very large focal length $2R = 25m$, where R is a Rowland circle radius (Fig.1), is one of the prime importance diagnostic instruments at Joint European Torus (JET) [3]. The ITER-oriented JET research program imposes a requirement on monitoring the impurity level of tungsten – the plasma-facing material of the new JET divertor. Therefore, besides the upgrade of the standard nickel monitoring using X-ray spectrometry, the functionality of the spectrometer should be extended towards tungsten impurity monitoring. New X-ray detection system optimized for Ni and W characteristic X-ray emission should be designed and constructed.

The main aim of the new X-ray diagnostic at JET is to provide the monitoring of the radiation emitted by Ni^{26+} and W^{46+} at 7.8keV and 2.4keV, respectively, from the hottest region of the JET plasma. The construction of the spectrometer allows one to extract two spectrally selected emission diapasons into the detection plane.

Characteristic emission lines could be measured independently using two detection units located behind the exit windows. The design of the position sensitive X-ray detector was driven by the following requirements: large detection area ($206 \times 92 mm^2$) matching the aperture of the single window of the spectrometer, good spatial resolution, high charge gain capability, detection stability for a wide range of photon rates and energy resolution capability (not worse than 30%). Multichannel proportional gas detectors are good candidates to fulfill the constraints. It has been demonstrated [4-6] that Gas Electron Multiplier (GEM) technique, when configured in multi-step structure, should provide sufficient detection characteristics.

2. TECHNICAL DESCRIPTION OF X-RAY GAS DETECTORS AND DETECTION EFFICIENCY

The construction of two detectors for highresolution X-ray diagnostics at JET is based on the Triple GEM (T-GEM) geometry [5] (Fig.2). The TGEM detectors should resolve energy and the position in the detection plane of the X-ray photons diffracted from the cylindrically bent crystals (see Fig.1). The T-GEM structure allows one to reach a high total gas gain (exceeding 104) with a very low

discharge probability. Due to strongly reduced space charge effects in the sequential amplification process a high rate capability can be achieved. The T-GEM structure with inter-GEM spacing of 2 mm and the induction gap width of 2.5mm should match the operational requirements of the JET high-resolution X-ray diagnostics. The single detector consists of 256 strips of 96mm length with 0.8mm pitch. It was demonstrated that the T-GEM detector filled with Ar/CO₂ gas mixture at atmospheric pressure provides a good charge gain and acceptable stability during medium-term operation.

An expanded view of the T-GEM detector and the assembled final T-GEM module are presented in Figs.3 and 4, respectively. As a construction material for detectors (frames and assembly bolts) Delrin material was chosen in order to avoid a secondary fluorescence. Standard GEM foils¹ were stretched and glued to the Delrin frames. The gas tightness is assured by o-rings placed between the frames.

Technology of the thin mylar window stretching and gluing to the dedicated frame assured good window flatness. The detector window was additionally supported by system consisting of two ribs installed on the outer side of the window. In this way good window flatness was assured when operated under small overpressure due to the gas circulation. The drift-gap frame and electrode frames have larger opening than the window frame that should reduce edge effects related to the electric field distortion in the vicinity of the dielectric surface. The strip plane on thick G-10 plate closes the gas volume. Gas mixture circulating in the sensitive volume is supplied through the inlets in the drift frame and the strip plate. Detectors for Ni and W monitoring at 7.8keV and 2.4keV, respectively have identical internal structure. The window thickness is smaller for low energy detector in order to increase detection efficiency in this energy range.

The AFE channel bandwidth is 15MHz matching timing characteristics of the primary pulse and the 100MHz sampling rate of digitization in the 10 bit ADCs. Dedicated algorithm of cluster size and cluster amplitude is implemented in the detection unit for the precise energy reconstruction.

The studies of the gas mixture and detector window materials have been performed in order to optimize the detection efficiency for selected energies of X-rays. The Ar/CO₂ (15%-30%) mixture with conversion layer thickness of 15mm has been chosen. In order to minimize the absorption in the window material, the technology of the thin (12µm and 5µm) aluminized mylar foil was chosen. The results of calculations of the detection efficiencies for Ni (with 12µm mylar window) and W (with 5µm mylar window) monitor X-ray detectors are shown in Fig.5. Detection efficiency above 40% for 2.4keV and around 20% for 7.8keV may be achieved.

The detector is mounted on the electronic crate containing amplifiers/shapers (AFE) (Fig.4). Analogue signals from strips are transmitted via special SMD connectors to the back-plane of the crate. Such installation assures good protection of the high voltage lines.

3. TECHNICAL DESCRIPTION OF ELECTRONICS

The detector electronics processing unit has 256 measurement channels [7] controlled by the signal processing unit. The single readout channel (Fig.6) consists of amplifier and differential cable driver, 10 bit Flash ADC of 100 MHz sampling. Readout channels are grouped by 16 in Analogue Front-End

¹ GEM foils were produced at CERN according to the standard technology developed there.

and FMC (FPGA Mezzanine Card) digital boards, respectively. Signals from each detector module are processed parallel by means of the custom FPGA processor. The aim of signals' processing is to estimate position distribution of X-ray hits on the strip plane with 50 time-slices per second. Two such processing units will be constructed for the 'low-energy' (2.4keV) and 'high-energy' (7.8keV) X-ray detectors.

The detector strip board is equipped with 256 strips connected to connectors which transfer signals to the backplane board. This board distributes detector signals to the AFE boards. It is attached to 3U Europa type crate where 16 AFE modules are plugged. The crate is mounted to the detector assembly. Each AFE module consists of 16 charge amplifiers followed by differential cable drivers equipped with MD5 connector. The cable driver converts single-ended signal from amplifier to differential one. Whole detector is supplied from dedicated T-GEM Power Supply Unit (PSU) which is customized version of commercially available product [8].

4. PROTOTYPE DETECTOR TESTS

Performance of the pulse reproduction precision by the FPGA system was established by comparison with digital scope recording with 2.5GHz sampling. The detector prototype with 10x10 cm² detection area and operated at nominal charge gain was irradiated by the ⁵⁵Fe source.

Figure 7 presents comparison of single-strip current signals of 8-bit resolution (1000 events) acquired with oscilloscope with 2.5GHz sampling (left) and the current signals of 10-bit resolution (1000 events) acquired with FPGA module with 100 MHz sampling (right). More technical details of this measurement can be found in Ref. [9].

The T-GEM X-ray prototype detector with 10x10cm² detection area was tested to study the performance of the detector for Ar/CO₂ (15-30%) gas mixture. Tests were performed by means of the ⁵⁵Fe X-ray source and 2.5kV X-ray generator providing narrow X-ray spectrum peaked at about 2keV.

Figure 8 shows the typical pulse-height spectrum measured with ⁵⁵Fe X-ray source (left) and X-ray generator (right), respectively. The 5.9keV X-ray peak is well separated from the escape peak of Ar. When selected detector area is irradiated simultaneously using the source and the generator delivering high intensity X-ray flux, linearity of the detector response is preserved with good energy resolution (below 17% FWHM). The ratio of fluxes corresponding to the source and the generator is reproduced in the measurement.

Single avalanches induced by X-rays are distributed over several strips of the read-out plane forming clusters. Mean multiplicity of clusters depends slightly on the X-ray energy in the given energy range. For the working voltages allowing full detection efficiency, the mean measured cluster multiplicity is about 3-4 strips, depending on the electric fields distribution in the amplification, transfer and induction stages. Hence, the position reconstruction is possible with "centre-of-gravity" method applied to the pulse-height distribution of individual clusters.

The position resolution was measured with collimated X-ray beam from the generator at 2.5kV. The spot of the photon flux was collimated down 0.7mm in diameter on the detector window.

The results of the measurement at two spot positions distant by 2mm are shown in Figure 9. The measurement has shown the local detector position resolution of 0.3 strip width (0.25mm).

The relative gain of the prototype detector filled with Ar/CO₂ (15-30%) was measured as a function of applied total GEM voltage by using the ⁵⁵Fe X-ray source. Total GEM voltage corresponds to the sum of voltages applied across the three GEMs. Results of these measurements at 1.2kV in the induction gap (Fig.10) indicate the monotonic dependence of the gain in the range of voltages applied. The increase of the charge gain with increasing voltage in the transfer gaps is also visible in the results presented.

In order to verify the operational stability of the detectors, a medium-term test has been performed. The charge gain and the energy resolution for the 5.9keV line were monitored. The energy resolution decreases (improves) from 25% to slightly below 20% within 75 hours. The significant dependence between gain and temperature-pressure ratio was also observed. Further tests are planned in order to obtain more precise information on this dependence.

SUMMARY

Two T-GEM detectors with 206×92 mm² detection area and 256 strip channels each were designed for both W⁴⁶⁺ (at 2.4keV) and Ni26+ (at 7.8keV) monitoring diagnostic channels on JET. Detectors will resolve energy and the position in the detection plane of the X-ray photons. In order to optimize the detection efficiencies studies of the gas mixture and detector window materials were performed. As material window and gas mixture the thin aluminized mylar (5μm and 12μm) and Ar/CO₂ (15-30%) were chosen and tested with the prototype detector. The expected detector efficiencies are 45% at 2.4keV (W monitoring channel) and 20% at 7.8keV (Ni monitoring channel), respectively. The energy resolution of 15%-17% and detection spatial resolution of 0.25 mm were obtained in preliminary testing measurements. Similar values are expected for final diagnostic X-ray detectors.

ACKNOWLEDGMENTS

This work was supported by EURATOM and carried out within the framework of the European Fusion Development Agreement. The views and opinions expressed herein do not necessarily reflect those of the European Commission. We also appreciate Didier Mazon for fruitful discussion.

REFERENCES

- [1]. K-D Zastrow, et al., *Journal of Applied Physics* **70**, 6732 (1991)
- [2]. K. W. Hill et al., *Review of Scientific Instruments* **79**, 10E320 (2008)
- [3]. R. Bartiromo, et al., *Review of Scientific Instruments* **60**(2), 237 (1989)
- [4]. A. Bressan et al., *Nuclear Instruments and Methods A* **424**, 321 (1999)
- [5]. C. Altunbas et al., *Nuclear Instruments and Methods in Physics Research A* **490**, 177 (2002)
- [6]. A. Kozlov et al., *Nuclear Instruments and Methods in Physics Research A* **523**, 345 (2004)
- [7]. G. Kasprowicz et al., *Proc. SPIE*, vol. 8008, 2011, 80080J
- [8]. www.creotech.pl
- [9]. K. Pozniak et al., *Proc. SPIE*, vol. 8008, 2011, 800808

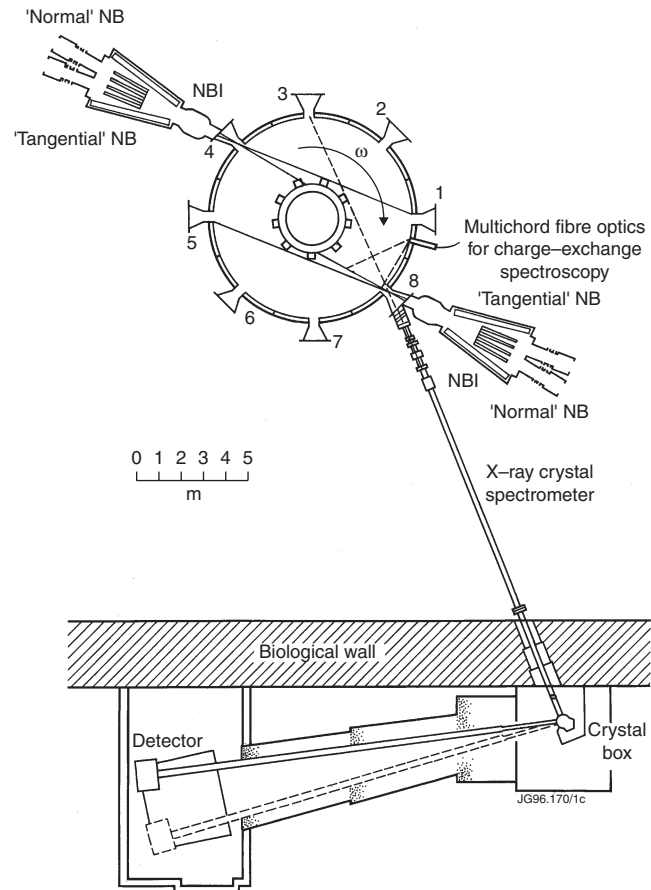


Figure 1: Layout of the high-resolution X-ray crystal spectrometer in the JET vacuum vessel

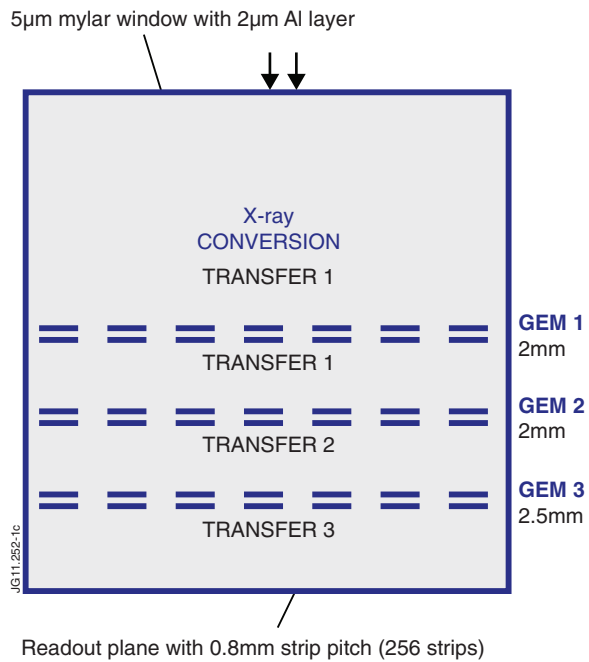


Figure 2: Scheme of the T-GEM detector structure

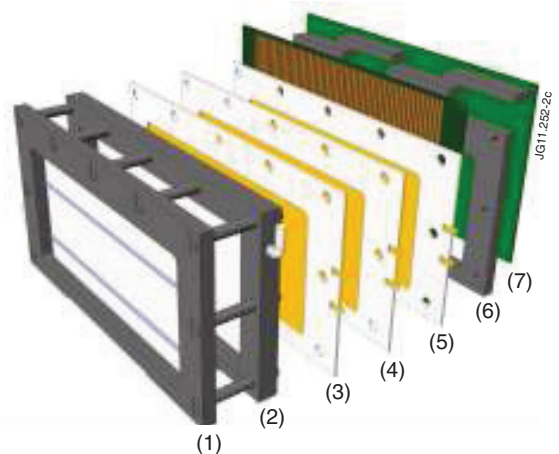


Figure 3: Structure of the T-GEM X-ray detector for JET diagnostics: (1) window frame, (2) drift-gap frame, (3)-(5) GEM foils with frames, (6) strip plane and (7) closing plane frame.

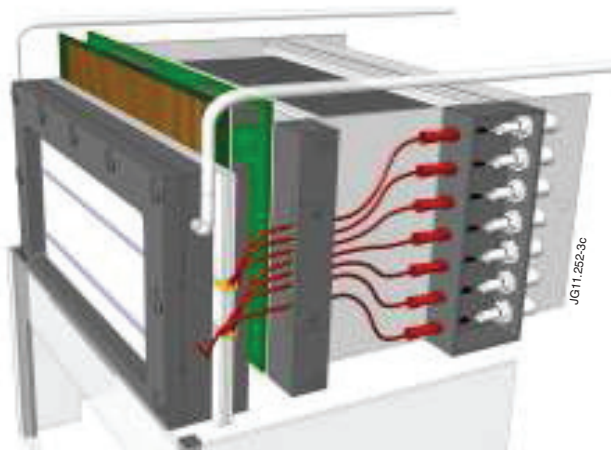


Figure 4: View of the assembled final T-GEM module.

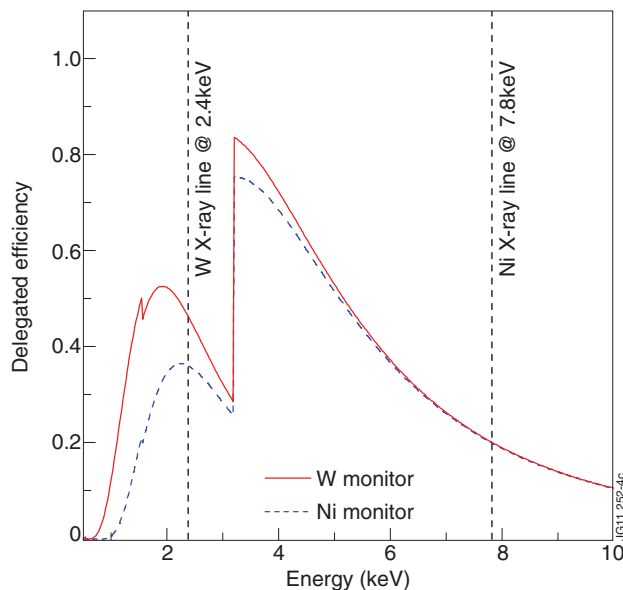


Figure 5: Calculated photon detection efficiencies as a function of photon energy for Ni and W monitor x-ray detectors with 12 μ m and 5 μ m mylar windows, respectively.

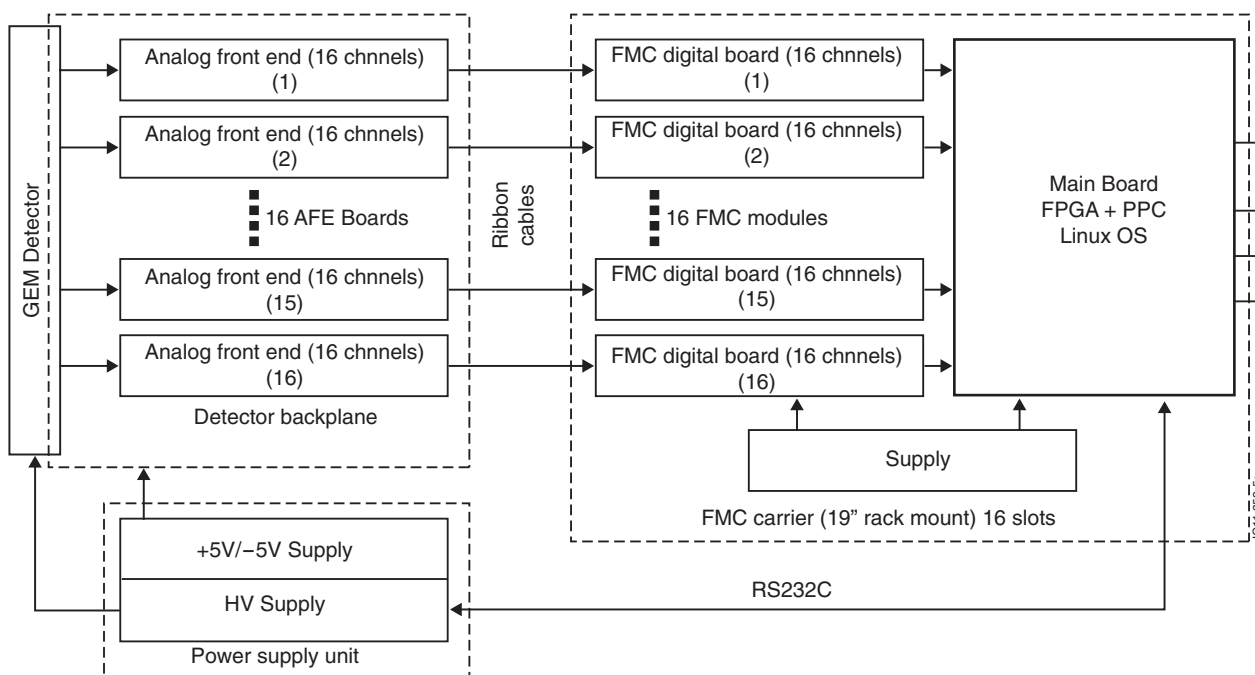


Figure 6: Processing electronics block schematic.

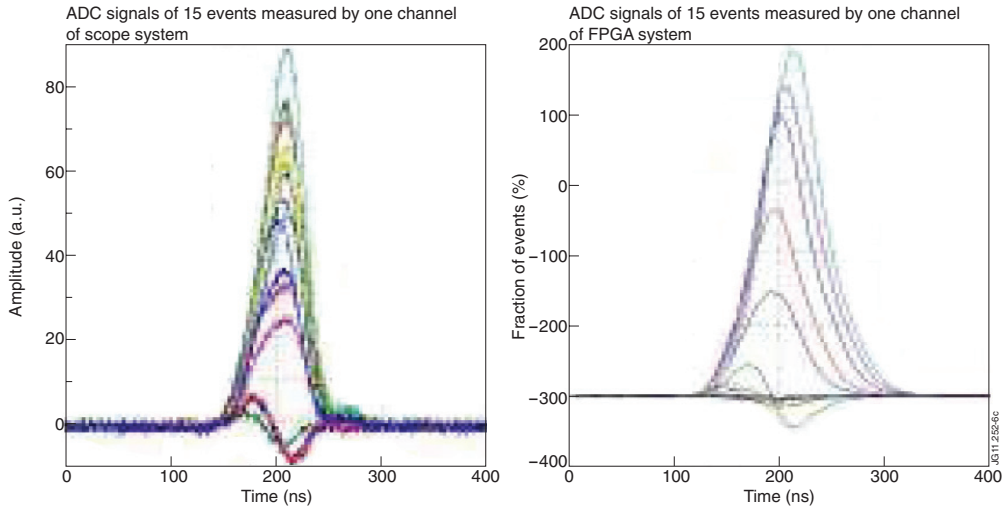


Figure 7: The anode current signals measured on one of the oscilloscope channel's (left) and the anode current signals for one channel using FPGA module (from two different measurements).

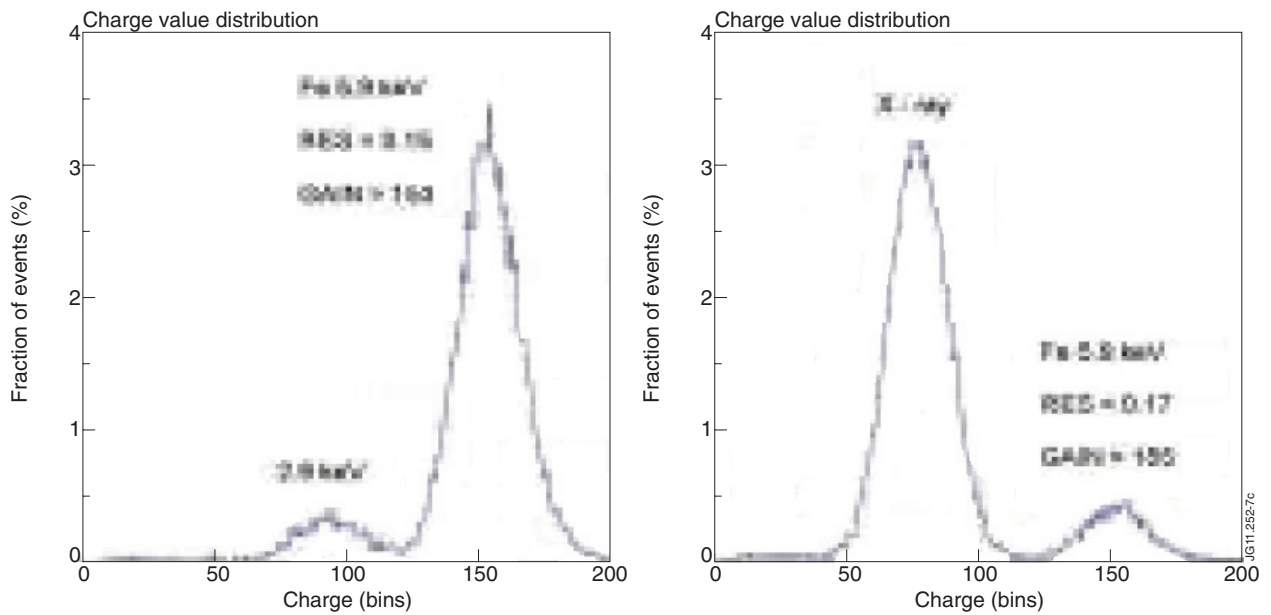


Figure 8: Charge (energy) distribution measured for a ^{55}Fe source (left) and for the 2.4kV X-ray tube and ^{55}Fe source together.

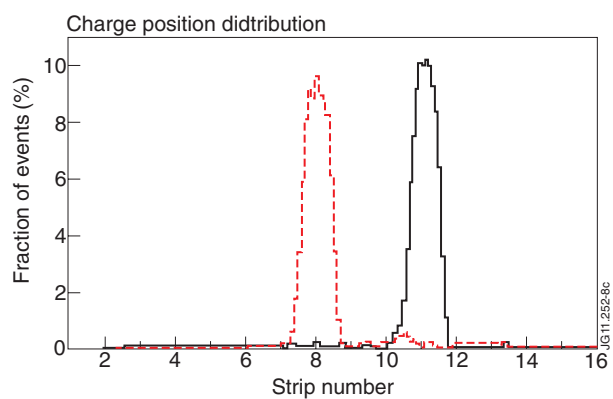


Figure 9: Charge position distribution for selected X-ray source position. X-ray tube (2.5kV, 100 uA) with a 0.7mm diameter collimator was used as a radiation source.

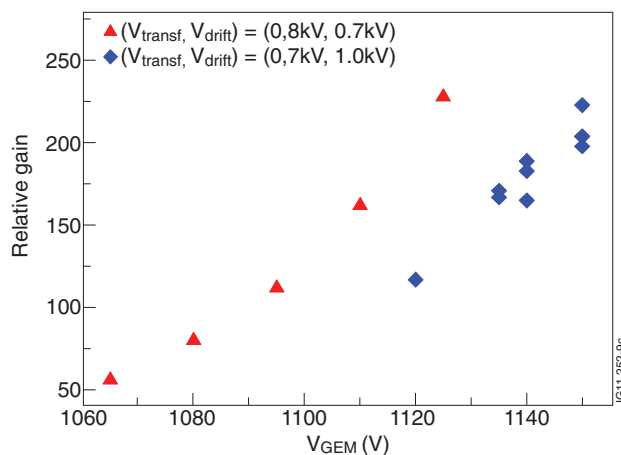


Figure 10: The relative gain versus the total GEM voltage.